

SUPERSONIC FLOW OVER A DIAMOND AIRFOIL

Eshant Shinde ¹

Department of Aerospace Engineering, Amity University Mumbai, Maharashtra, India - 410206

Mentor : Biraj Khadka ²

FOSSEE, IIT-Bombay, Mumbai, Maharashtra, India - 400076

Mentor : Evan Fernandes³

FOSSEE, IIT-Bombay, Mumbai, Maharashtra, India - 400076

Guide : Dr. Tushar Chourushi ⁴

Assistant Professor, Department of Aerospace Engineering, MIT-ADT University, Pune, India - 412201

ABSTRACT

The objective of this work is to study the aerodynamic characteristics of a "Double-Wedge" airfoil at supersonic speeds using the SonicFoam solver in. The study is divided into two parts: (1) In the first part, an analytical solution is obtained; and (2) in the second part, CFD simulations are performed using OpenFOAM. The work involves obtaining analytical results such as Mach number, pressure, temperature around the airfoil, oblique shock angle, expansion wave, and drag and lift coefficients. Additionally, Mach number, pressure, and temperature contours are captured to visualize the flow behavior around the airfoil. The analytical results are then compared with simulation data to identify differences for further study. A mesh independence study was also conducted to determine the optimal mesh size for accurate results. Figure 1 below shows the geometry of the double-wedge airfoil, with the dimensions specified. The airfoil has a length of 1 meter and a half-wedge angle of 5 degrees.

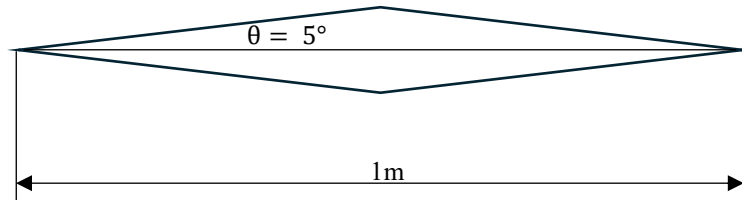


Figure 1 : Geometry of Double-Wedge Airfoil

Contents

Introduction	1
Overview of an Aerodynamics effect at Supersonic conditions	2
2.1 Introduction	2
2.2 Classification of Shock waves	2
2.2.1 Normal Shock	2
2.2.2 Oblique Shock	3
2.2.3 Bow Shock	3
2.2.4 Conical Shock	3
2.2.5 Expansion Fan / Prandtl-Meyer Expansion	3
Part 1 : Analytical solution	4
3.1 Governing equations	4
3.2 Analytical study of a Double-Wedge airfoil	7
Theory	11
4.1 Governing Equations.....	11
4.2 Geometry.....	11
4.3 Meshing	12
4.4 Solver Setup	13
4.5 Mesh Independence Study	15
Results & Discussion	16
5.1 Case study of the Analytical & simulation Results	16
5.2 Coefficient of Drag (Cd) & Lift (Cl) variation with Angle of Attack	17
5.3 Velocity over Double-Wedge Airfoil	19
5.4 Pressure Contours of Double-Wedge Airfoil	21
.....	22
5.5 Temperature Contours of Double-Wedge Airfoil	23
Conclusion.....	25

Introduction

A diamond-shaped airfoil, also known as a double-wedge airfoil, is commonly used in supersonic blades and wings due to its sharp leading and trailing edges. Supersonic airfoils come in two main types: double-wedge and biconvex. Both designs feature sharp edges at the leading and trailing points and have a symmetrical appearance, which makes them less efficient at low angles of attack [1][4]. The aerodynamic phenomena that occur around these airfoils, such as shock formation, are further classified into "normal shocks" and "oblique shocks." Additionally, expansion waves are observed when the flow turns in a way that causes it to expand in the direction of the flow. Expansion waves consist of multiple shockwaves occurring at the same point in the flow [2][3].

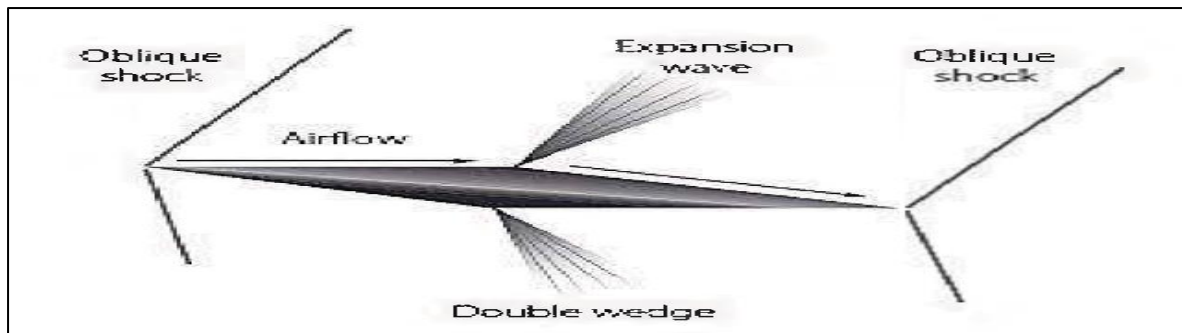


Figure 2 : Double-Wedge Airfoil Geometry with Oblique Shock and Expansion Fan [4]

The double-wedge airfoil is highly efficient under supersonic conditions but performs less effectively at subsonic speeds. Despite this, it remains a valuable tool for researchers who use it in numerical analyses, validation studies, and data collection at various Mach numbers, including hypersonic speeds (Mach 5 or higher). This airfoil design helps in understanding complex fluid behavior near the airfoil boundary, as well as shock generation and interaction at supersonic speeds. As humanity continues to seek faster means of travel, the exploration of supersonic travel has become more feasible in the modern era, bringing us closer to achieving speeds beyond the sound barrier.

One of the first notable studies on double-wedge airfoils was conducted by researchers such as Adolf Busemann, a German engineer known for his work on supersonic aerodynamics. Busemann's work in the 1930s laid the groundwork for the use of double-wedge airfoils in high-speed aircraft design. The studies became particularly significant during World War II and the subsequent Cold War era, when supersonic flight was a major focus for military and aerospace research [8].

Overview of an Aerodynamics effect at Supersonic conditions

2.1 Introduction

The term "supersonic" refers to the condition when the speed of an object or fluid exceeds the speed of sound, which is 343.2 m/s. This phenomenon is often expressed in terms of the Mach number 'M' [2]. At supersonic speeds, the aerodynamic behavior of objects undergoes significant changes due to the effects of compressibility. As an object surpasses the speed of sound, the surrounding air is unable to move out of the way quickly enough, leading to the formation of shockwaves. These shockwaves cause sudden changes in pressure, temperature, and density [2].

The flow in supersonic conditions becomes highly non-linear, meaning that even small changes in speed or shape can lead to significant alterations in flow patterns. The shockwaves generated at these speeds are categorized into different types, including normal shocks, oblique shocks, bow shocks, and expansion fans. The presence of these shockwaves increases drag and alters aerodynamic forces, affecting lift, drag, and the center of pressure, which in turn impacts stability and control [2][3].

When designing vehicles or missiles for supersonic conditions, these phenomena must be carefully considered. [6] Key aspects such as material selection, aerodynamic design, shockwave management, thermal management, propulsion systems, and drag reduction are critical for ensuring performance and safety in supersonic flight.

2.2 Classification of Shock waves

Shockwaves are a type of propagating disturbance in a medium, typically characterized by an abrupt, nearly discontinuous change in pressure, temperature, and density. They occur when a wave travels faster than the local speed of sound in the medium, causing the energy to compress into a thin region, leading to a rapid change in the medium's properties [2][3].

Technically, shockwaves are solutions to the nonlinear hyperbolic partial differential equations governing fluid dynamics, such as the Euler equations. They are characterized by a sudden increase in entropy, making them irreversible and distinct from ordinary sound waves, which are linear and reversible. Shockwaves can occur in various contexts, including supersonic flight, explosions, and even in astrophysical events.

2.2.1 Normal Shock

A normal shock is a type of shock wave that occurs perpendicular to the direction of flow in a supersonic fluid, typically air. Unlike oblique shocks, where the shock wave is angled relative to the flow, a normal shock wave is perfectly perpendicular. This results in a sudden and drastic change in the flow properties across the shock. The key characteristics of a Normal Shock is flow speed reduction, pressure, temperature, density increases. While normal shocks are fundamental to the study of supersonic aerodynamics, they also represent a source of

inefficiency. The significant loss of kinetic energy across a normal shock leads to a corresponding increase in entropy, meaning that the process is irreversible [2][3]. Therefore, engineers often seek to manage or minimize normal shocks to improve the efficiency of high-speed flight systems.

2.2.2 Oblique Shock

Oblique shock waves are a type of shock wave that forms when a supersonic flow encounters a change in the flow direction, typically caused by a physical object like a wedge or an airfoil. Unlike normal shock waves, which occur perpendicular to the flow direction, oblique shock waves are inclined at an angle to the flow [2][3].

Conditions for an Oblique Shock formation such as the incoming flow must be supersonic ($M > 1$), flow deflection angle, Mach number it is dependent on incoming flow, higher the Mach numbers lead to stronger shock waves with more significant changes in pressure, temperature and flow direction and at last the admissible deflection angle, its deflection angle must be withing certain limits for an oblique shock to form. If the angle is too large, the shock wave can detach from the surface and form detached bow shock, which is a more complex flow structure.

2.2.3 Bow Shock

A bow shock is a curved shock wave that forms in front of an object moving at supersonic speeds, such as the nose of spacecraft or a blunt body. It occurs when the supersonic flow encounters a blunt object, causing the shock wave to curve around the object. Bow shocks form around reentry vehicles, blunt-nosed missiles, and supersonic aircraft [2][3].

2.2.4 Conical Shock

Conical Shocks form when a supersonic flow encounters a sharp, pointed, or conical object, such as the nose of a missiles or a high-speed aircraft. As the flow impacts the conical surface, it is compressed and deflected, resulting in the formation of a shock wave that emanates from the point of the cone and spreads outward in a conical shape. This type of shock wave is characterized by its three-dimensional nature, as opposed to the two-dimensional characteristics of planar shocks [2][3].

2.2.5 Expansion Fan / Prandtl-Meyer Expansion

Expansion Fan or Prandtl-Meyer Expansion is not a shock but is related and often discussed in conjunction with shocks. It is a series of expansion waves that occurs when supersonic flow turns around a convex corner. Since Expansion Fan are isentropic there is decrease in pressure, temperature and density but increase in Mach number. An expansion fan consists of an infinite

number of infinitesimally weak expansion waves that spread out from the point where the flow turns [2][3].

Part 1 : Analytical solution

3.1 Governing equations

The behaviour of flow before & after the normal shock is governed by the conservation equation [2]

1. Conservation of Mass :

$$\rho_1 u_1 = \rho_2 u_2 \quad (1)$$

Where ρ_1 & ρ_2 are the densities before and after the shock, and u_1 & u_2 are the velocities before and after the shock.

2. Conservation of Momentum :

$$P_1 + \rho_1 u_1^2 = P_2 + \rho_2 u_2^2 \quad (2)$$

Where P_1 & P_2 are the pressure before and after the shock.

3. Conservation of Energy :

$$h_1 + \frac{u_1^2}{2} = h_2 + \frac{u_2^2}{2} \quad (3)$$

Where h_1 & h_2 are the specific enthalpies before and after the shock.

4. Mach number relation before and after the shock can be obtained by [2][12]:

$$M_2^2 = \frac{1 + \left[\frac{(\gamma-1)}{2}\right] M_1^2}{\gamma M_1^2 - \frac{(\gamma-1)}{2}} \quad (4)$$

Where γ is the specific heat ratio and usually taken as ($\gamma = 1.4$ for air).

The rise in pressure, temperature and density ratio downstream a normal shock can be calculated using the following equations [2][12]:

$$\frac{P_2}{P_1} = 1 + \frac{2\gamma}{\gamma+1} (M_1^2 - 1) \quad (5)$$

$$\frac{\rho_2}{\rho_1} = \frac{u_1}{u_2} = \frac{(\gamma+1)M_1^2}{(\gamma-1)M_1^2+2} \quad (6)$$

$$\frac{T_2}{T_1} = \left(\frac{p_2}{p_1}\right) \left(\frac{\rho_2}{\rho_1}\right) \quad (7)$$

The following relation for the Oblique shock are as follows [2]:

Shock Angle is the angle between the direction of the incoming flow and the shock wave. The deflection angle θ , which is the angle where the flow turns and the shock angle is represented by β .

Mach number before the shock M_1 & after the shock M_2 are related by the shock angle. The θ - β -M relationship is given by the following equation [2][12]:

$$\tan(\theta) = 2\cot(\beta)\left(\frac{M_1^2 \sin^2(\beta) - 1}{M_1^2(\gamma + \cos(2\beta) + 2)}\right) \quad (8)$$

where : θ = deflection angle

β = shock angle

M_1 = upstream mach number

γ = specific heat ratio

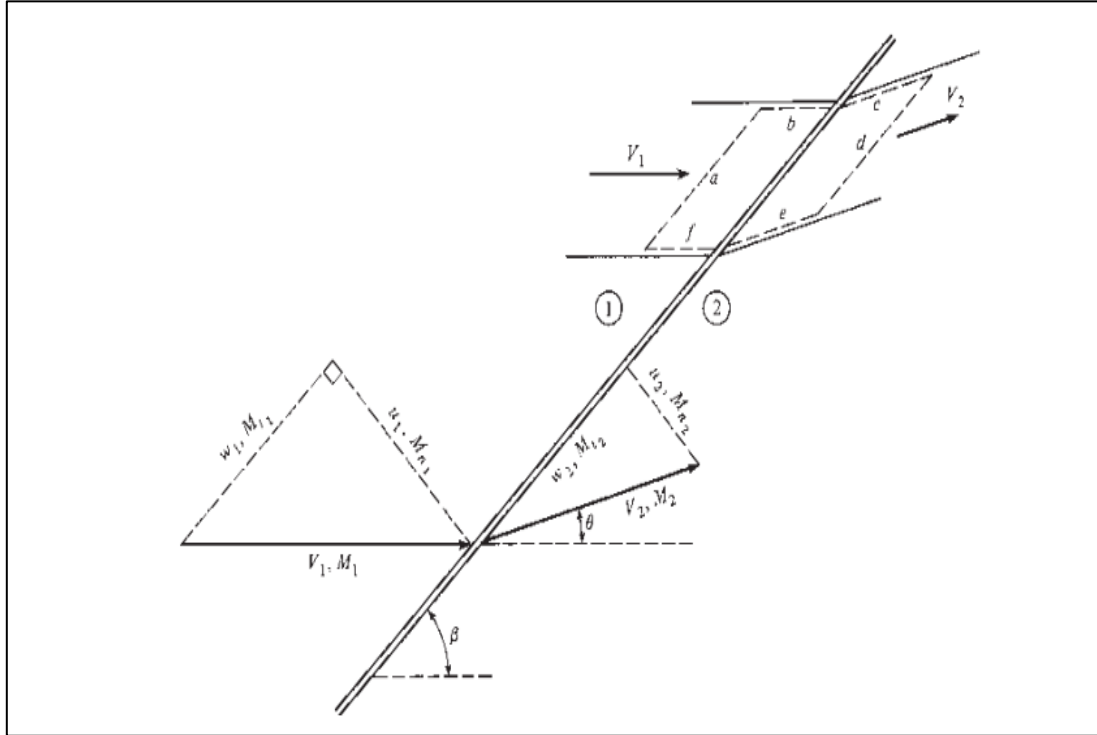


Figure 3 : Oblique Shock wave geometry [2]

Changes across an oblique shock in terms of the normal component of the upstream Mach number M_{n1} . That is, for an oblique shock wave with

$$M_{n1} = M_1 \sin \beta \quad (9)$$

To calculate the Mach number after the oblique shock wave M_2 can be found from M_{n2} and it's shown in the figure x :

$$M_2 = \frac{M_{n2}}{\sin(\beta - \theta)} \quad \text{or} \quad = \frac{M_2 \sin(\beta)}{\sin(\beta - \theta)} \quad (10)$$

To calculate the pressure, density and temperature after an oblique shock as follows :

$$\frac{p_2}{p_1} = \frac{1+2\gamma}{\gamma+1} (M_1^2 \sin^2(\beta) - 1) \quad (11)$$

$$\frac{\rho_2}{\rho_1} = \frac{(\gamma+1)M_1^2 \sin^2(\beta)}{(\gamma-1)M_1^2 \sin^2(\beta)+2} \quad (12)$$

$$\frac{T_2}{T_1} = \left(\frac{p_2}{p_1}\right) \left(\frac{\rho_2}{\rho_1}\right) \quad (13)$$

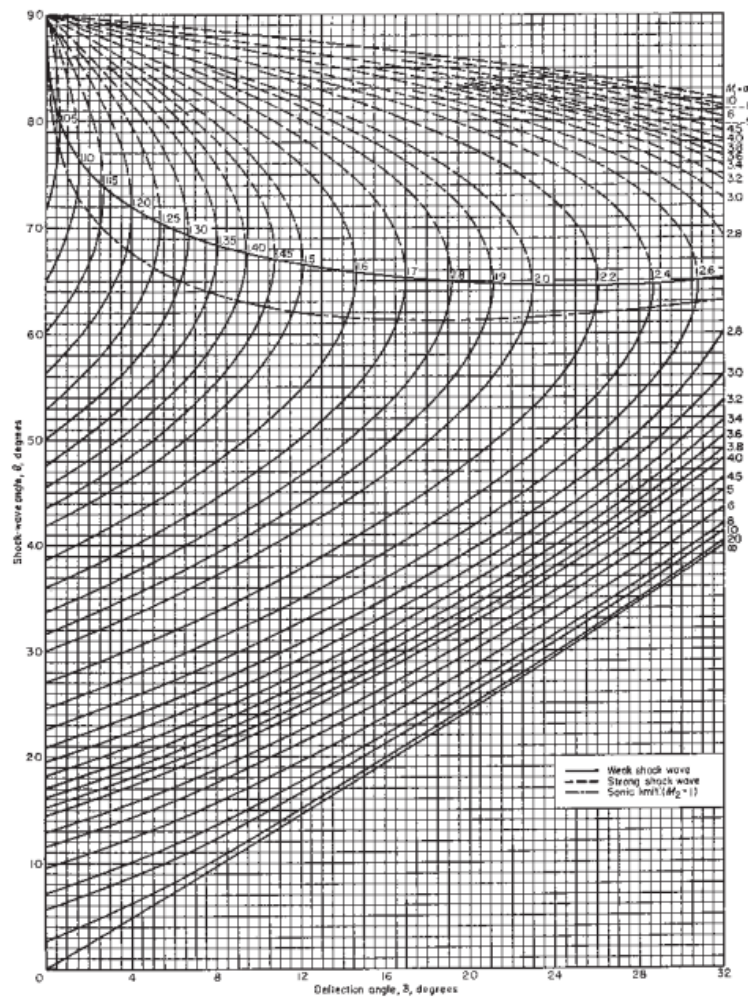


Figure 4 : Oblique Shock properties for ($\gamma = 1.4$) [2]

The following relation for the Expansion Fan or Prandtl-Meyer Expansion as follows :

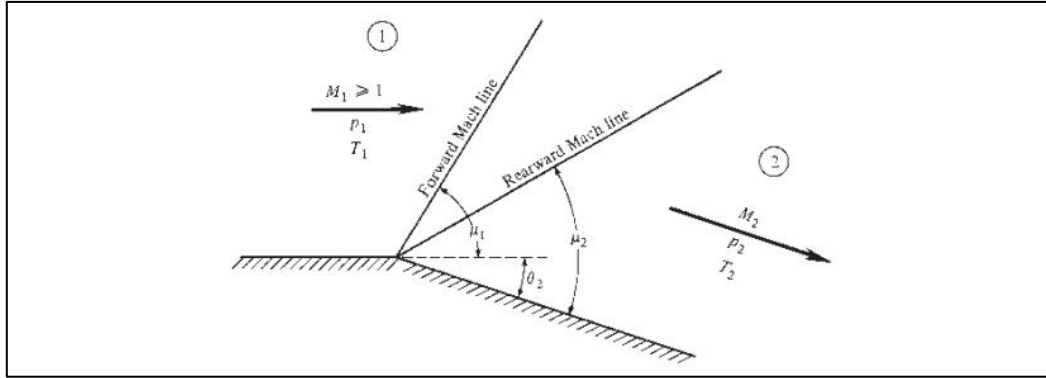


Figure 5 : Expansion Fan or Prandtl-Meyer Function wave geometry [2]

1. Prandtl – Meyer Function

$$v(M) = \sqrt{\frac{\gamma+1}{\gamma-1}} \tan^{-1} \left(\sqrt{\frac{\gamma-1}{\gamma}} (M^2 - 1) \right) - \tan^{-1}(\sqrt{M^2 - 1}) \quad (14)$$

Where,

M = is the Mach number of the flow

γ = is the specific heat ratio of the gas (1.4 for air)

2. Turning Point (θ)

The turning angle is the angle through which the flow has turned as it passes through the expansion fan. This angle is directly related to the change in the Prandtl-Meyer function [12].

If the flow turns from Mach number M_1 to M_2 the turning angle θ is given by :

$$\theta = v(M_2) - v(M_1) \quad (15)$$

3. The expansion fan itself is a continuous expansion region, composed of an infinite number of Mach waves, bounded upstream by μ_1 and downstream by μ_2 where,

$$\mu_1 = \sin^{-1} \left(\frac{1}{M_1} \right) \quad (16)$$

$$\mu_2 = \sin^{-1} \left(\frac{1}{M_2} \right) \quad (17)$$

3.2 Analytical study of a Double-Wedge airfoil

In this report the numerically solve calculation performed on the double-wedge airfoil at different Mach number (1.4, 2.4 & 3.4) at 0° Angle of Attack through which the values obtain will be compared with the simulation results. Results such as Mach number after the oblique shock wave and Expansion fan, shock angle, pressure, density and temperature.

Case 1 : Oblique Shock

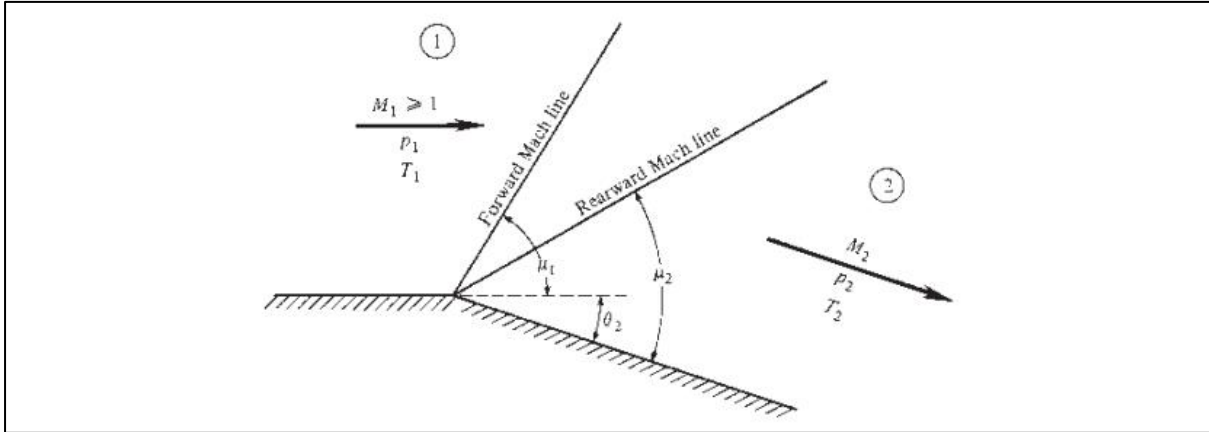


Figure 6 : Oblique Shock wave geometry [2]

First to find the Shock angle (β) using the $\theta - \beta - M$ chart from Figure 4 for the deflection angle of ($\theta = 5^\circ$) $\beta = 52.78$. Thus,

$$Mn_1 = M_1 \sin \beta = 1.4 \times \sin (52.78) = 1.1148$$

Using the Normal Shock properties for $Mn_1 = 1.1148$:

$$\frac{p_2}{p_1} = 1.2832 \quad \frac{T_2}{T_1} = 1.2832 \quad \frac{\rho_2}{\rho_1} = 1.2832$$

we get,

$$Mn_2 = 0.9004$$

Thus for,

$$p_2 = \frac{p_2}{p_1} p_1 = 130.0405 \text{ kPa}$$

$$T_2 = \frac{T_2}{T_1} T_1 = 320.1414 \text{ K}$$

$$\rho_2 = \frac{\rho_2}{\rho_1} \rho_1 = 1.4632 \text{ kg/m}^3$$

we get,

$$M_2 = \frac{Mn_2}{\sin (\beta - \theta)} = \frac{0.9004}{\sin (52.74 - 5)} = 1.2158$$

Case II : Expansion Fan / Prandtl – Meyer Function

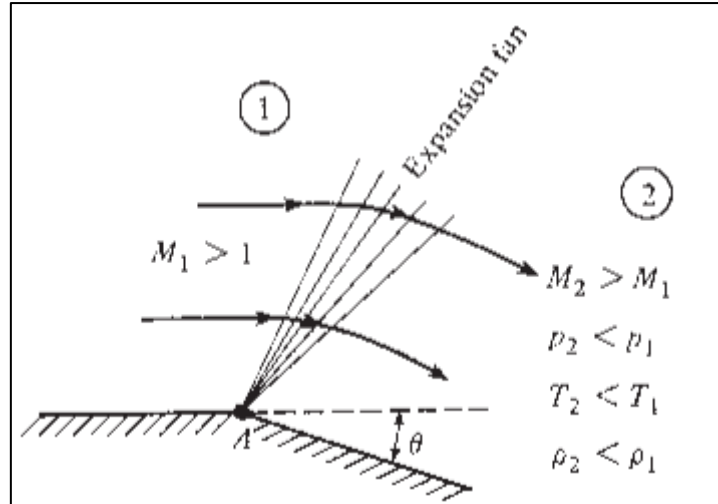


Figure 7 : Expansion Fan wave geometry [2]

Using Prandtl-Meyer Function Table :

$$v(M_1) = 21.30$$

Therefore,

$$\theta = v(M_2) - v(M_1)$$

$$5 = v(M_2) - 21.30$$

$$\therefore v(M_2) = 26.30$$

$$\therefore M_2 = 1.9985$$

Now, using M_2 & M_3 value to find μ_1 & μ_2

$$\mu_1 = \sin^{-1} \left(\frac{1}{M_2} \right) = \sin^{-1} \left(\frac{1}{1.8213} \right) = 33.30$$

$$\mu_2 = \sin^{-1} \left(\frac{1}{M_2} \right) = \sin^{-1} \left(\frac{1}{1.9985} \right) = 30.24$$

$$\text{Expansion fan angle } (\alpha_{\text{fan}}) = \mu_1 - \mu_2 + \theta_2 = 33.30 - 30.24 + 5 = 8.06$$

Since, expansion fan are isentropic, using isentropic table to obtain P_o & T_o are constant through the wave.

Here P_{o1} & P_{o2} is equal same to $T_{o2} = T_{o1}$.

$$P_2 = 103.3190 \text{ kPa}$$

$$T_2 = 299.777 \text{ K}$$

$$\rho_2 = 1.2415 \text{ kg/m}^3$$

The above example is how the numerical calculations are performed to obtain the results for the double-wedge airfoil.

Hence, for the rest of the Mach number (2.4 & 3.4)

TABLE 1 : Calculated values of Oblique Shock and Expansion Fan

Mach 2.4				
Sr no.	Pressure, (kPa)	Temperature, (K)	Density, (kg/m³)	Mach no. (M)
1.	101.325	298	1.225	2.4
2.	138.430	326.07	1.529	2.19
3.	101.444	298.36	1.224	2.38

β	μ		α_{fan}
	μ_1	μ_2	
28.53	27.169	24.748	7.421

TABLE 2 : Calculated values of Oblique Shock and Expansion Fan

Mach 3.4				
Sr no.	Pressure, (kPa)	Temperature, (K)	Density, (kg/m³)	Mach no. (M)
1.	101.325	298	1.225	3.4
2.	153.811	336.442	1.646	3.10
3.	101.452	298.7	1.222	3.38

β	μ		α_{fan}
	μ_1	μ_2	
20.70	18.819	17.185	6.634

Theory

4.1 Governing Equations

The SonicFoam solver in OpenFOAM is a transient solver for simulating compressible flows, particularly in scenarios involving high speeds, such as transonic and supersonic flows. It is equipped to handle the changes in density that occur in these flows and can model the effects of shock waves. SonicFoam also incorporates RAS (Reynolds-Averaged Stress) turbulence models to approximate turbulence in the flow, making it suitable for engineering problems where capturing the overall flow behavior is more critical than resolving every detail of the turbulence [13][14].

SonicFoam solves the compressible Navier-Stokes equations, which include :

1. Continuity Equation (Conservation of Mass) :

$$\frac{\partial \rho}{\partial t} + \nabla \cdot (\rho \mathbf{u}) = 0 \quad (18)$$

where ρ is the fluid density and \mathbf{u} is the velocity vector.

2. Momentum Equation (Conservation of Momentum) :

$$\frac{\partial (\rho \mathbf{u})}{\partial t} + \nabla \cdot (\rho \mathbf{u} \mathbf{u}) = -\nabla p + \nabla \cdot \boldsymbol{\tau} + \rho \mathbf{g} \quad (19)$$

Where p is the pressure $\boldsymbol{\tau}$ is the stress tensor, and \mathbf{g} represents body forces like gravity.

3. Energy Equation (Conservation of Energy) :

$$\frac{\partial (\rho E)}{\partial t} + \nabla \cdot (\rho E \mathbf{u}) = \nabla \cdot (k \nabla T) + \boldsymbol{\tau} : \nabla \mathbf{u} - \nabla : \mathbf{q} \quad (20)$$

Where E is the total energy per unit mass, (T) is temperature, (k) is the thermal conductivity, and \mathbf{q} is the heat flux.

4. Equation of State (Ideal Gas Law, if applicable) :

$$p = \rho R T \quad (21)$$

where R is the specific gas constant.

4.2 Geometry

The modelling design of the Double-Wedge Airfoil was created using the OpenFOAM's blockMesh file. For this particular project, simple rectangular domain was selected and the geometry is considered as 2-dimensional model. And all the simulations run on different AOA (Angle of Attack) are performed using the geometry model without any changes.

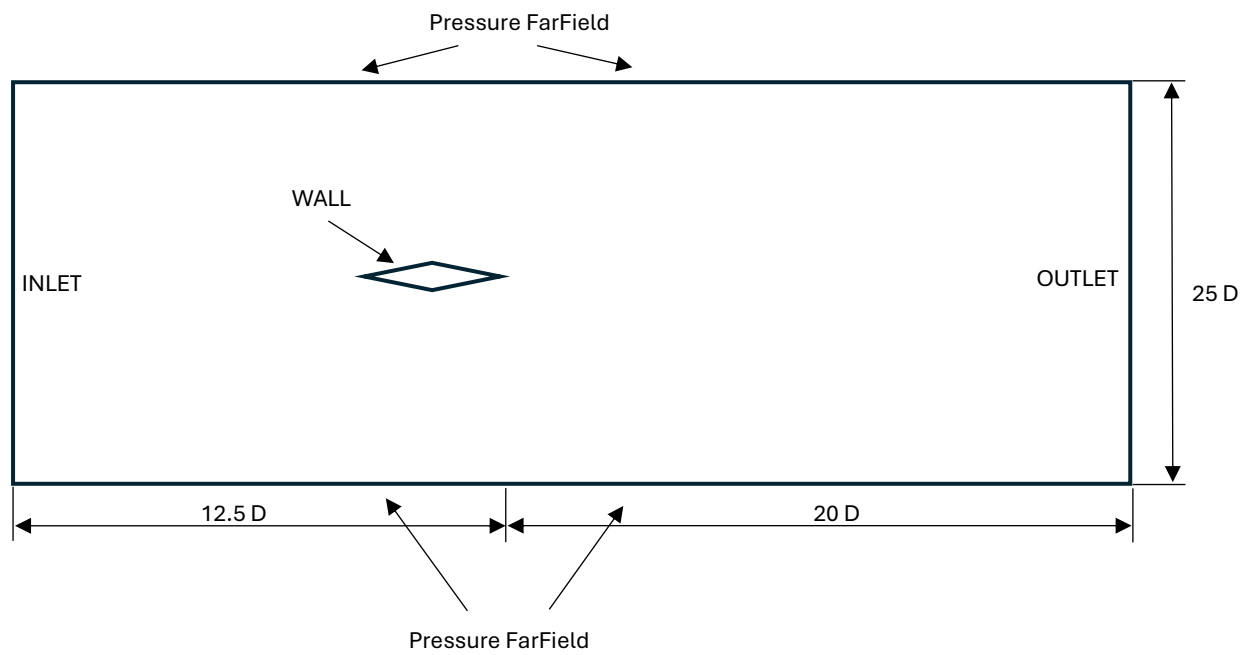
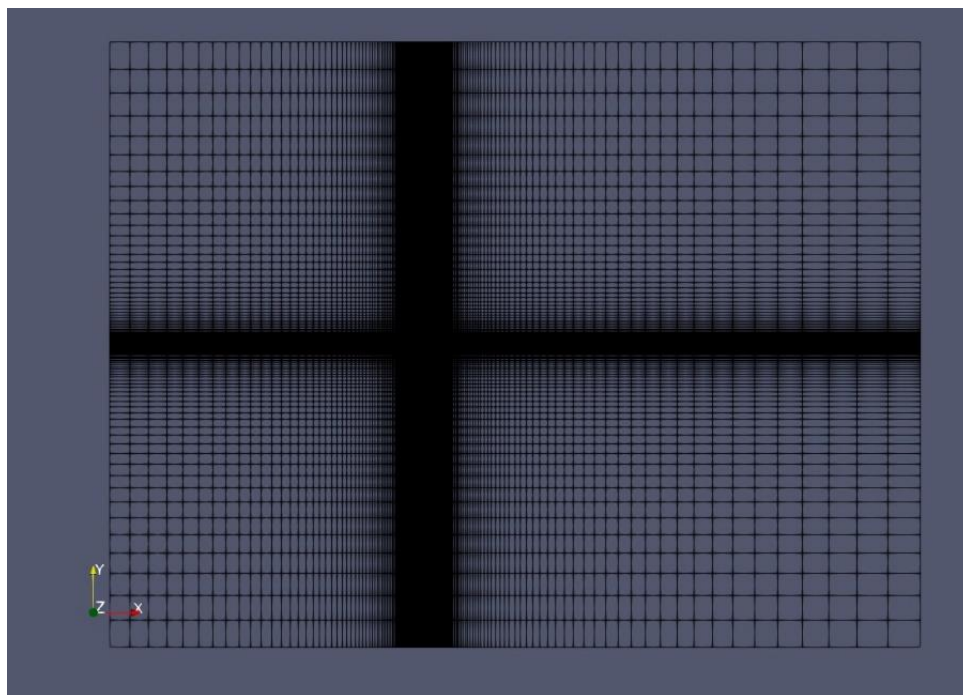


Figure 8 : Computational domain and boundary conditions

4.3 Meshing



Figuring 9 : Grid Mesh for Double-Wedge Airfoil

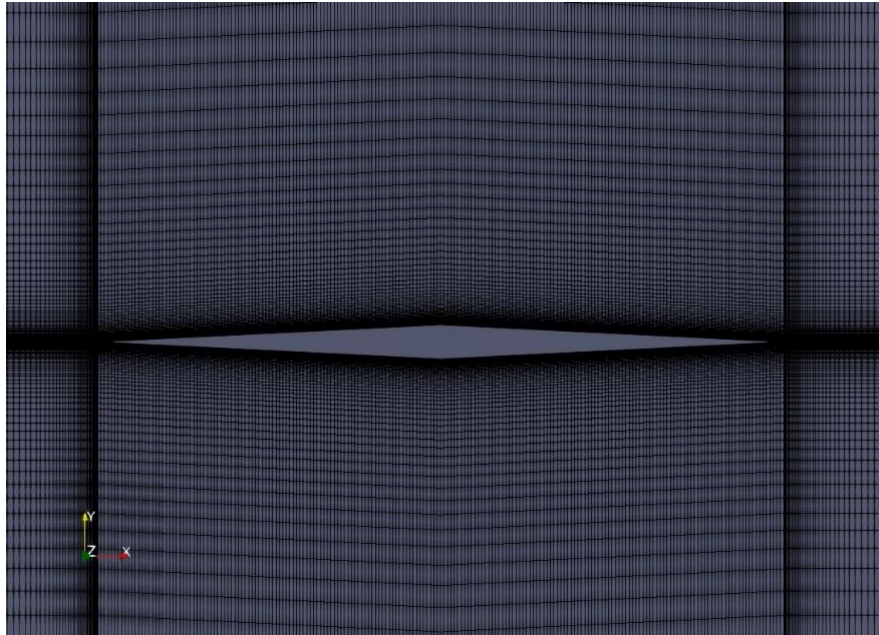


Figure 10 : Detail visualization of Mesh

Structured meshes were produced for this geometry in OpenFOAM's blockMesh. The total number of 80k cells were produced.

4.4 Solver Setup

For this project as mentioned earlier there are total three Mach number (1.4, 2.4 & 3.4) for the Double-Wedge airfoil. For this the constant parameters for this case are as follows:

Table 3 : Constant Parameters

PARAMETERS	VALUES
Pressure	101.325 kPa
Temperature	298 K
Density	1.225 kg/m ³

The following boundary conditions including the turbulence conditions and the type of patch name use for this case as follows :

Table 4 : Boundary Conditions

Variable	Inlet	Outlet	Bottom	Top	Wall
P	FixedValue	WaveTransmissive	Zerogradient	zerogradient	Zerogradient
T	FixedValue	inletOutlet	inletOutlet	inletOutlet	Zerogradient
u	FixedValue	inletOutlet	supersonicFreestream	supersonicFreestream	noSlip
α_T	Calculated	Calculated	Calculated	Calculated	alphatwallFunction
k	FixedValue	inletOutlet	inletOutlet	inletOutlet	kqwallFucntion
ϵ	FixedValue	inletOutlet	inletOutlet	inletOutlet	epsilonwallFunction
nut	Calculated	Calculated	Calculated	Calculated	nutwallFunction

Since the cases involve different angles of attack, the flow velocity angle changes rather than altering the entire geometry. The flow velocity in the x and y directions is adjusted accordingly, and the following equations are used to calculate these changes:

For x-direction :

$$= u \cos(\theta) \quad (22)$$

For y-direction :

$$= u \sin(\theta) \quad (23)$$

Where, u is the freestream velocity and θ is the value of angle of attack.

Here, are the values obtained from the above equations :

Table 5 : Velocity for Resolution at Mach 1.4

Mach No. 1.4 (480.2 m/s)		
Angle of Attack (θ)	Resolution of Velocity (m/s)	
	X	y
5	478.372	41.692
10	472.904	83.387
15	463.837	124.284

Table 6 : Velocity for Resolution at Mach 2.4

Mach No. 2.4 (823.2 m/s)		
Angle of Attack (θ)	Resolution of Velocity (m/s)	
	X	y
5	819.868	71.746
10	810.693	142.947
15	795.150	213.059

Table 7 : Velocity for Resolution at Mach 3.4

Mach No. 3.4 (1166.2 m/s)		
Angle of Attack (θ)	Resolution of Velocity (m/s)	
	x	Y
5	1161.176	101.641
10	1148.482	202.508
15	1126.462	301.834

4.5 Mesh Independence Study

A mesh independence study is a critical procedure in numerical simulations, especially in fields like Computational Fluid Dynamics (CFD). It is performed to ensure that the accuracy of the simulation results is not overly dependent on the discretization of the computational domain, commonly referred to as the mesh. The mesh is a grid of elements or cells that divides the domain into smaller, manageable sections where the governing equations are solved numerically. The accuracy of the results can be affected by the size and quality of these mesh elements. If the mesh is too coarse (i.e., the elements are too large), the simulation might not capture the necessary details of the physical phenomena being model, leading to inaccurate results. On the other hand, if the mesh is too fine (i.e., the elements are very small), while the results may be more accurate, the computational cost (in terms of time and resources) can become prohibitively high [4].

The mesh independence study involved several steps, including adjusting the element size and refining the mesh near the airfoil. Initially, the mesh consisted of 20k elements, and with each iteration, the number of elements was increased by 20k, as illustrated in the figure below. Multiple simulations were conducted, and the coefficients of drag (C_d) and lift (C_l) were obtained to compare the results across different mesh configurations. During the study, a sudden decrease in C_d was observed at 40k elements, followed by a gradual increase. From 80k to 140k elements, the C_d values stabilized, indicating convergence. Consequently, a mesh size of 80k elements was deemed the optimal choice for the final case, balancing accuracy and computational efficiency. The below figure shows the variation in Co-efficient of Drag as the elements size or cells increased.

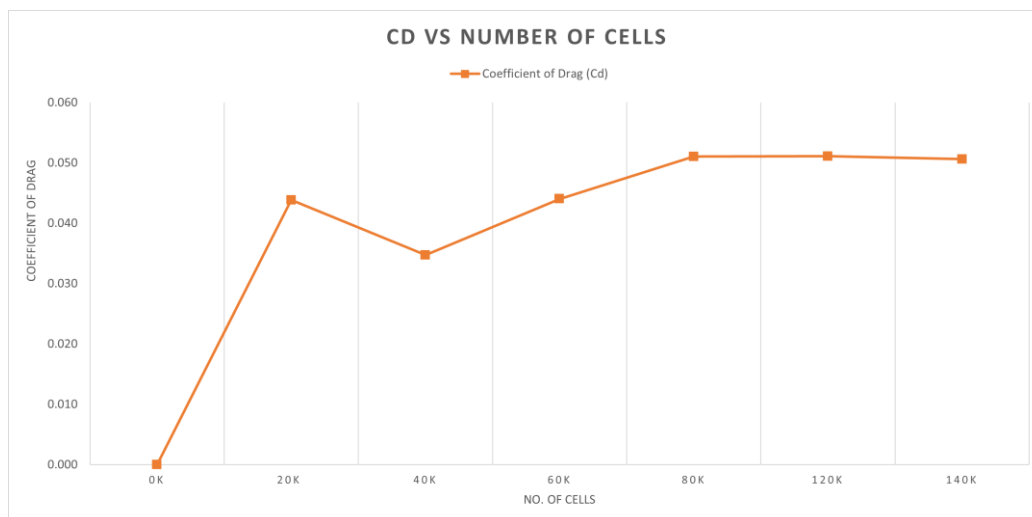


FIGURE 11 : Mesh Independence study plot

Results & Discussion

For this project, numerical data including pressure, temperature, density, and Mach number were obtained around the airfoil as the Mach number increased with varying angles of attack. Additionally, comparisons of the Coefficient of Drag (C_d) and Coefficient of Lift (C_l) are shown, along with visualizations of fluid flow and shock wave generation. The calculated numerical results, shown in Tables 1 and 2, are compared with the simulation results to assess the error. It is important to note that the numerical analysis was conducted solely at a 0-degree angle of attack for all Mach numbers.

5.1 Case study of the Analytical & simulation Results

The numerical results obtained for the double-wedge airfoil have been validated and are shown in the figure 23 below. These results, derived from the analytical study and the simulation performed using the SonicFoam solver, include Mach number, pressure, and temperature. These will be compared to evaluate the differences between the two sets of data.

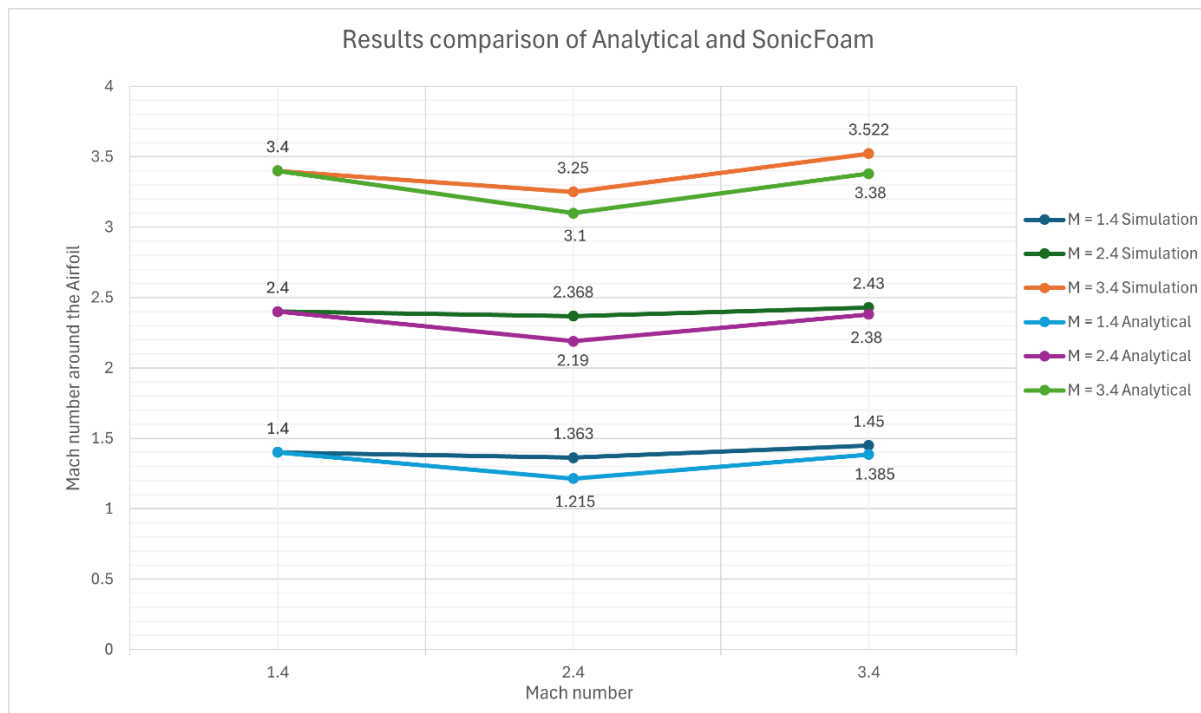


Figure 23 : Mach number plots of Analytical study and SonicFoam solver results at 0 degree AOA

The above plots shows the change in Mach number as the freestream velocity passes over the Double-wedge airfoil at 0 degree Angle of Attack (AOA). Figure 23 shows the calculation from Analytical study and SonciFoam simulation results.

Table 8 : Pressure and Temperature results after Oblique Shock at 0° AOA

Oblique Shock		
	Analytical	Simulation

Mach No.	Pressure (kPa)	Temperature (K)	Density (kg/m ³)	Pressure (kPa)	Temperature (K)	Density (kg/m ³)
1.4	130.040	320.141	1.463	112.741	300.442	1.180
2.4	138.430	326.071	1.529	812.274	302.992	1.372
3.4	153.811	336.442	1.646	124.546	308.85	1.451

Table 9 : Pressure and Temperature results after Expansion Fan at 0° AOA

Expansion Fan						
Mach No.	Analytical			Simulation		
	Pressure (kPa)	Temperature (K)	Density (kg/m ³)	Pressure (kPa)	Temperature (K)	Density (kg/m ³)
1.4	103.319	299.777	1.241	498.029	295.041	1.061
2.4	101.444	298.36	1.224	86.857	288.833	1.123
3.4	101.452	298.7	1.222	85.421	281.041	1.313

The differences between the analytical and SonicFoam results suggest that while the simulation is generally accurate, there are areas for improvement. Refining the mesh, adjusting numerical schemes, validating boundary conditions, exploring different turbulence models, and conducting time-step sensitivity analyses can help minimize these discrepancies and improve the accuracy of the simulations.

5.2 Coefficient of Drag (Cd) & Lift (Cl) variation with Angle of Attack

After the simulation the values obtained for Cd and Cl are compared with Mach 1.4, 2.4 & 3.4 as angle of attack increase.

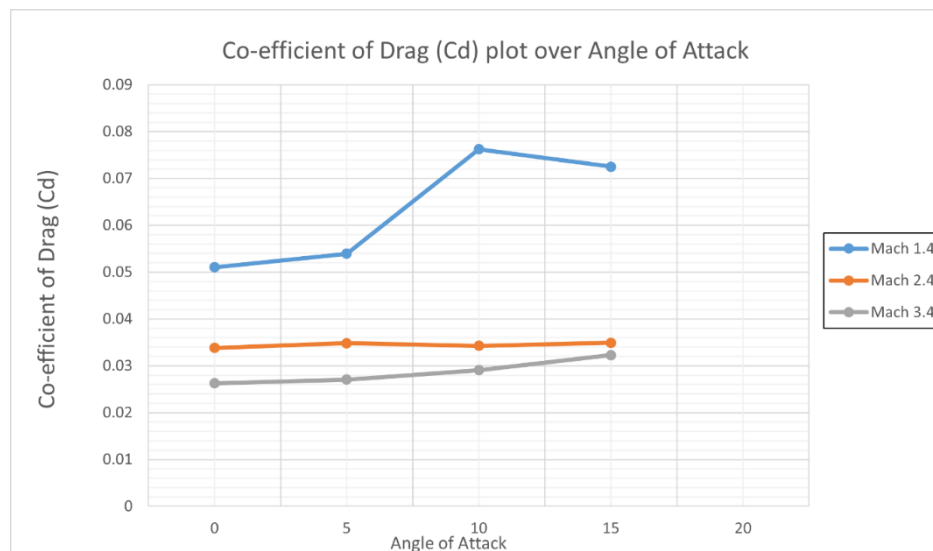


FIGURE 12 : Coefficient of Drag (Cd) variation with increase in Angle of attack

As shown above, the Coefficient of Drag (C_d) remains constant with the increase in free-stream velocity. However, it increases with a rise in the angle of attack, which is to be expected.

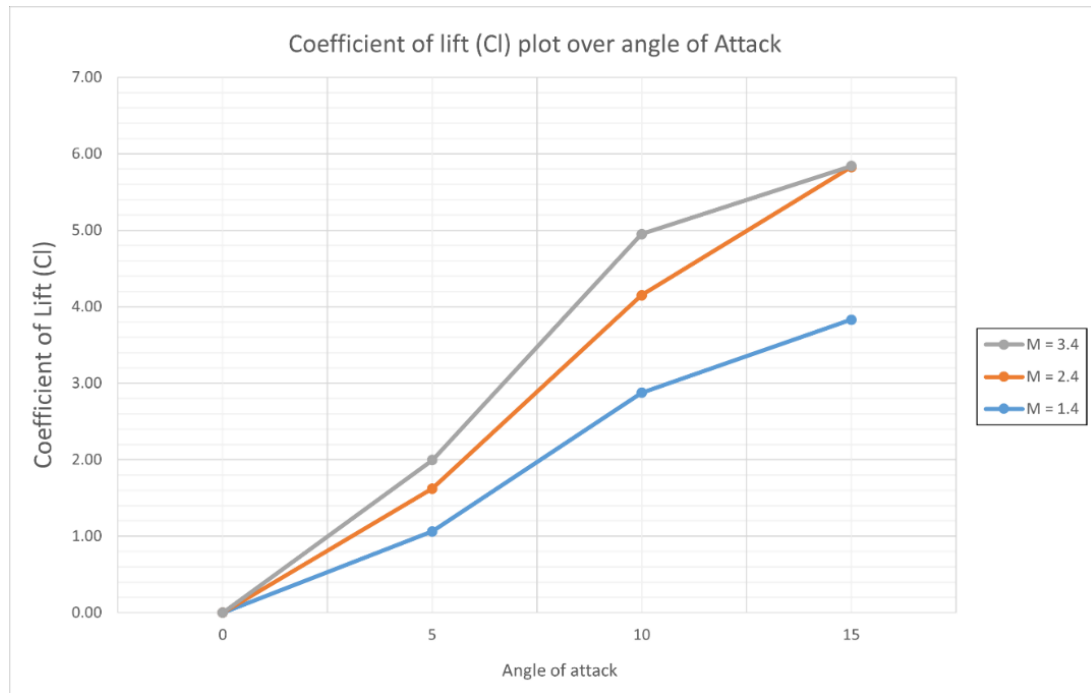


FIGURE 13 : Coefficient of Lift (C_l) variation with increase in Angle of Attack

Here, the Coefficient of Lift (C_l) is shown varying with changes in the angle of attack and increasing Mach number. As demonstrated, lift increases with the angle of attack; here, lift is greater at higher Mach numbers and less at lower Mach numbers which is.

5.3 Velocity over Double-Wedge Airfoil

Mach number remains constant before and after the airfoil, but as the airfoil passes through it, significant changes in Mach number are seen due to shock formation and expansion fan. As the Angle of Attack changes the leading edge start to experience Expansion Fan over it's top and Oblique Shock at it's bottom. Mach number decreases as it pass through oblique shock and increases as it goes through expansion fan. All this same phenomenon are seen in this case. From the contours shown below, it is evident that as the Mach number increases, the oblique shock angle reduces.

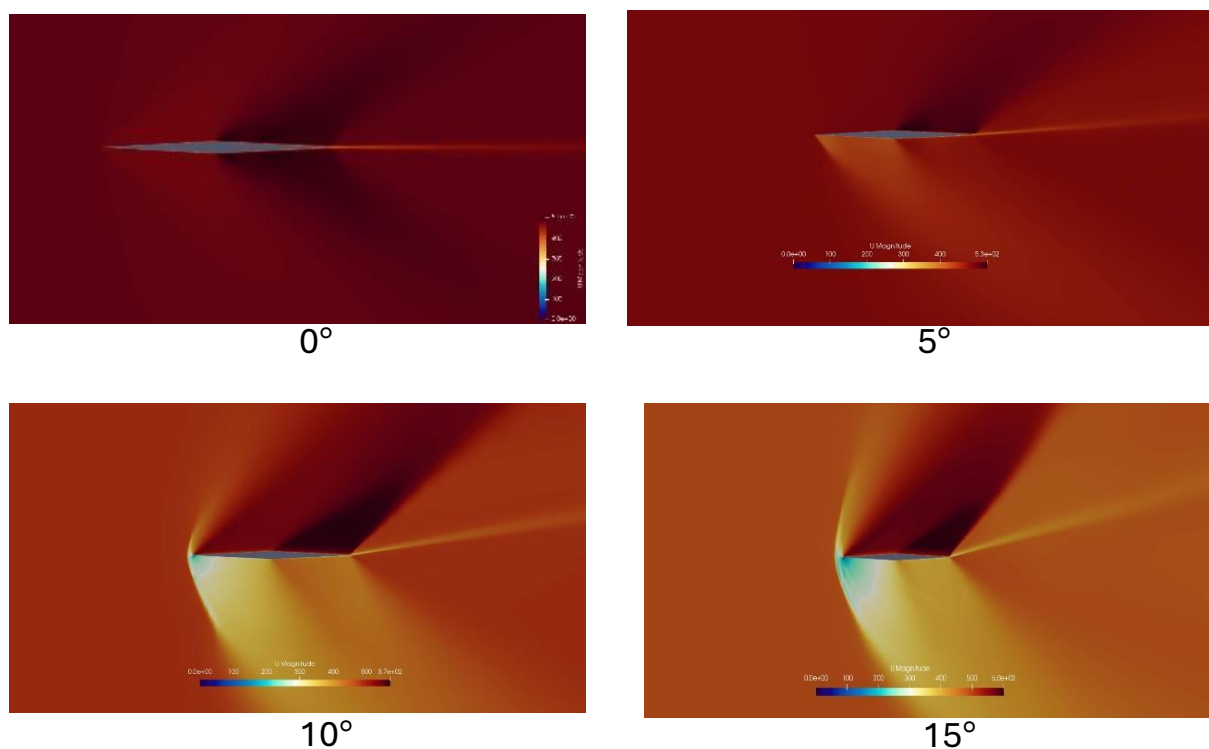
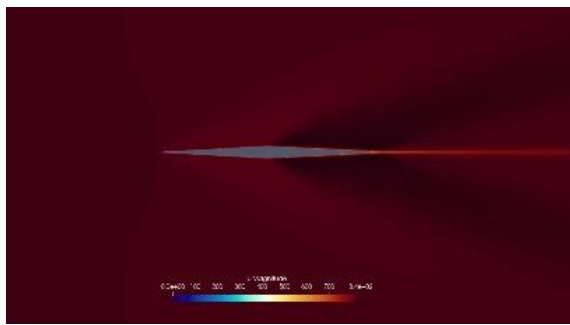
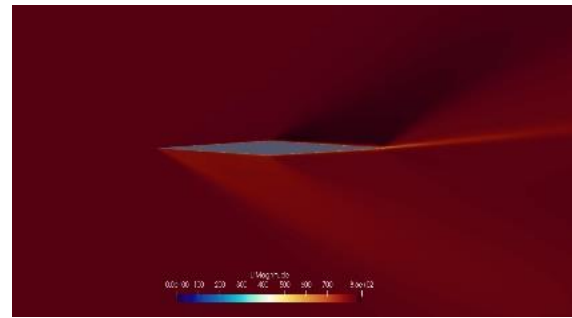


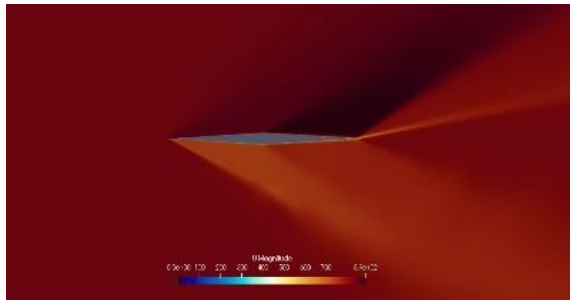
FIGURE 14 : Velocity contour for Mach 1.4 at different Angle of Attack



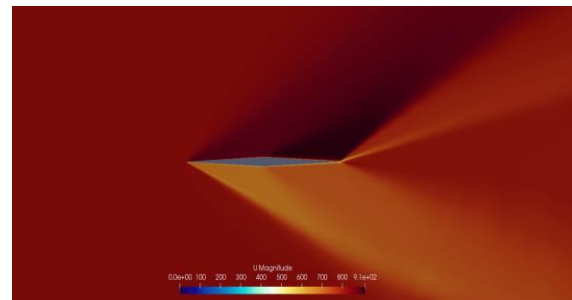
0°



5°

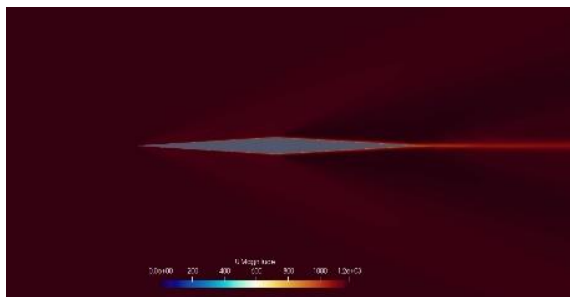


10°

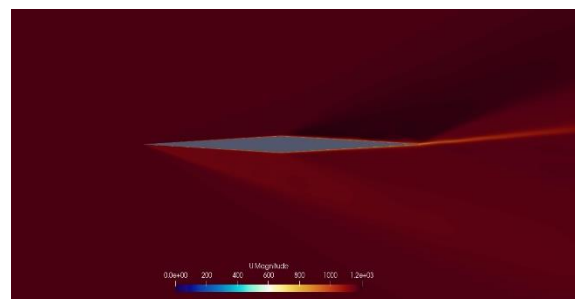


15°

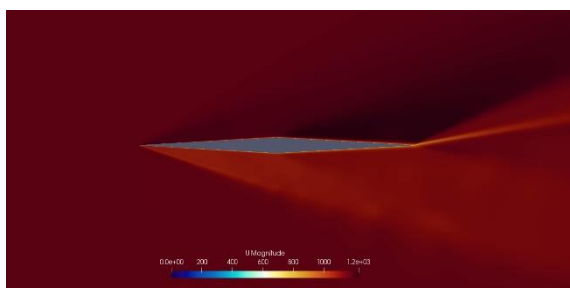
FIGURE 15 : Velocity contour for Mach 2.4 at different Angle of Attack



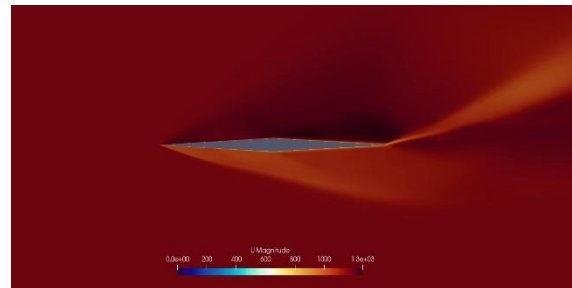
0°



5°



10°



15°

FIGURE 16 : Velocity contour for Mach 3.4 at different Angle of Attack

5.4 Pressure Contours of Double-Wedge Airfoil

Here, the pressure remains constant before and after the airfoil passes through the region. However, across the oblique shock, the pressure increases and then decreases as it passes through the expansion fan. A double-wedge airfoil experiences the highest pressure at the leading edge, particularly at the stagnation point, when it is at an angle of attack during supersonic speeds. This occurs because the airflow encounters sharp deceleration and compression, leading to a significant increase in pressure. The leading-edge shock wave, which forms due to the supersonic flow, further contributes to this pressure spike. The distribution of pressure around the double-wedge airfoil has been previously shown. In the given figure below, it is clearly evident that the pressure above the airfoil is lower and the pressure below the airfoil is higher.

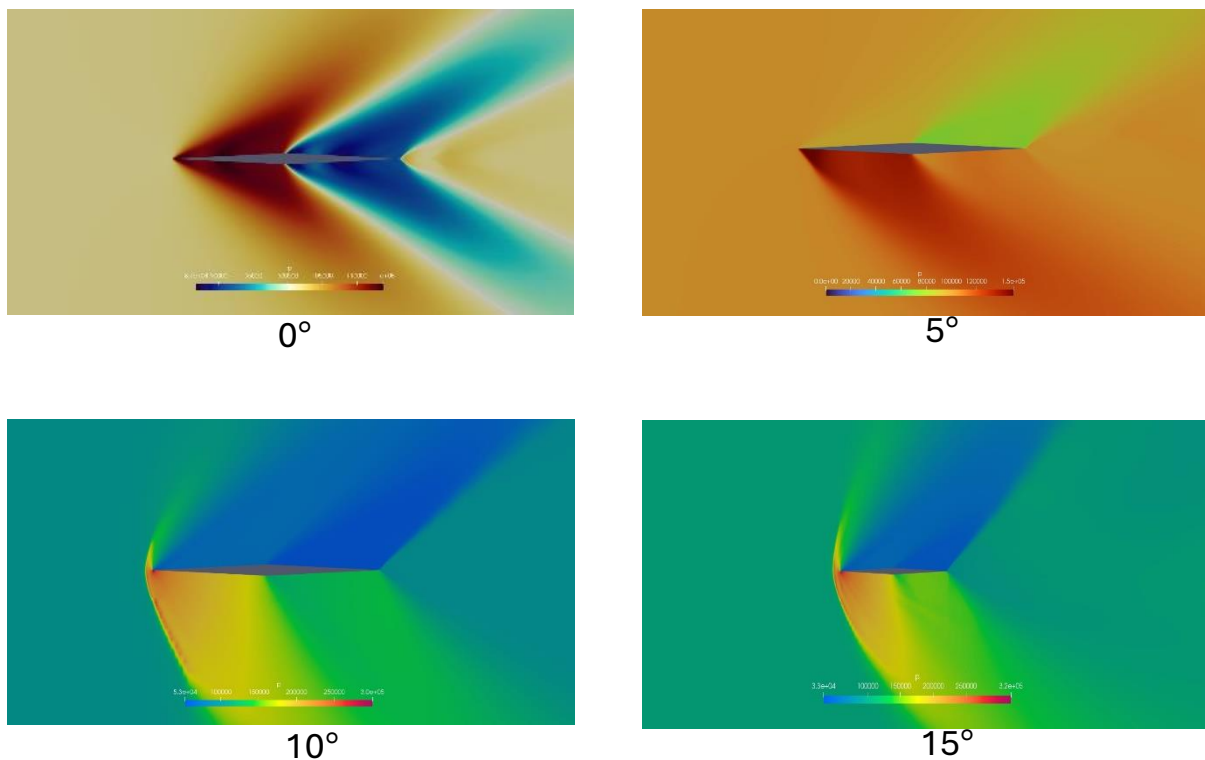


FIGURE 17 : Pressure contour for Mach 1.4 at different Angle of Attack

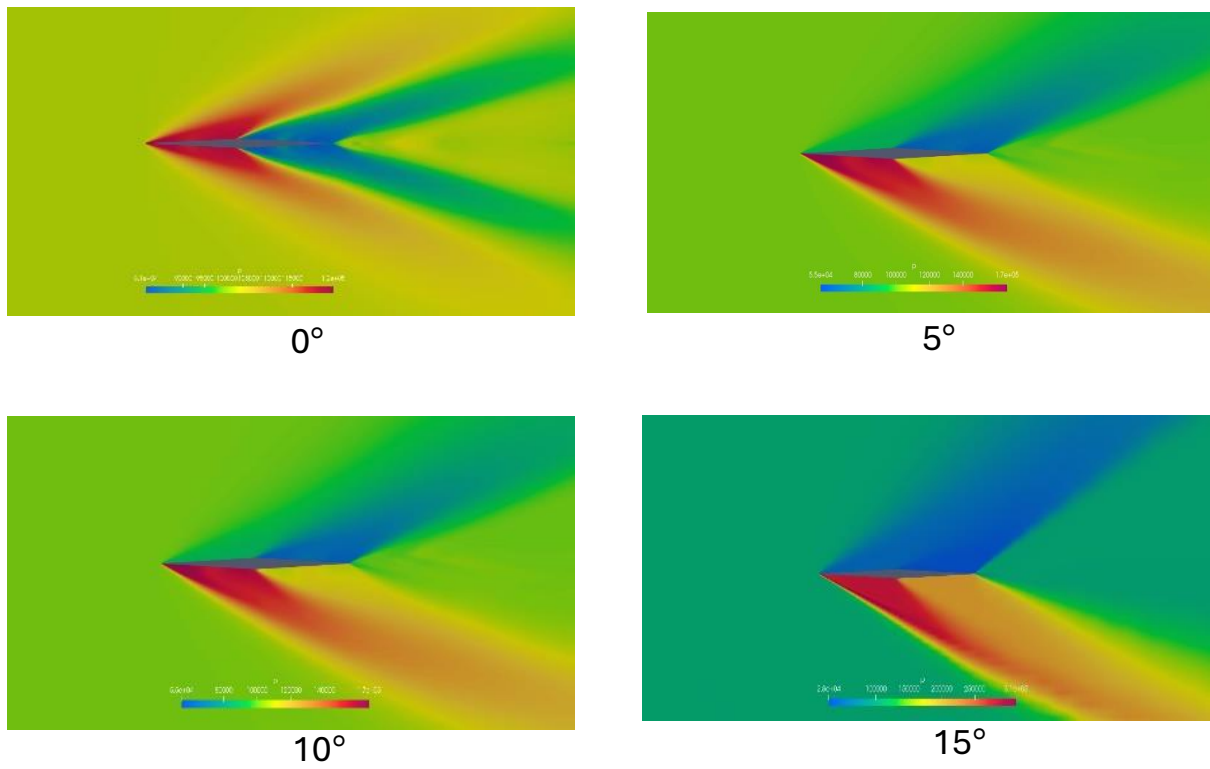


FIGURE 18 : Pressure contour for Mach 2.4 at different Angle of Attack

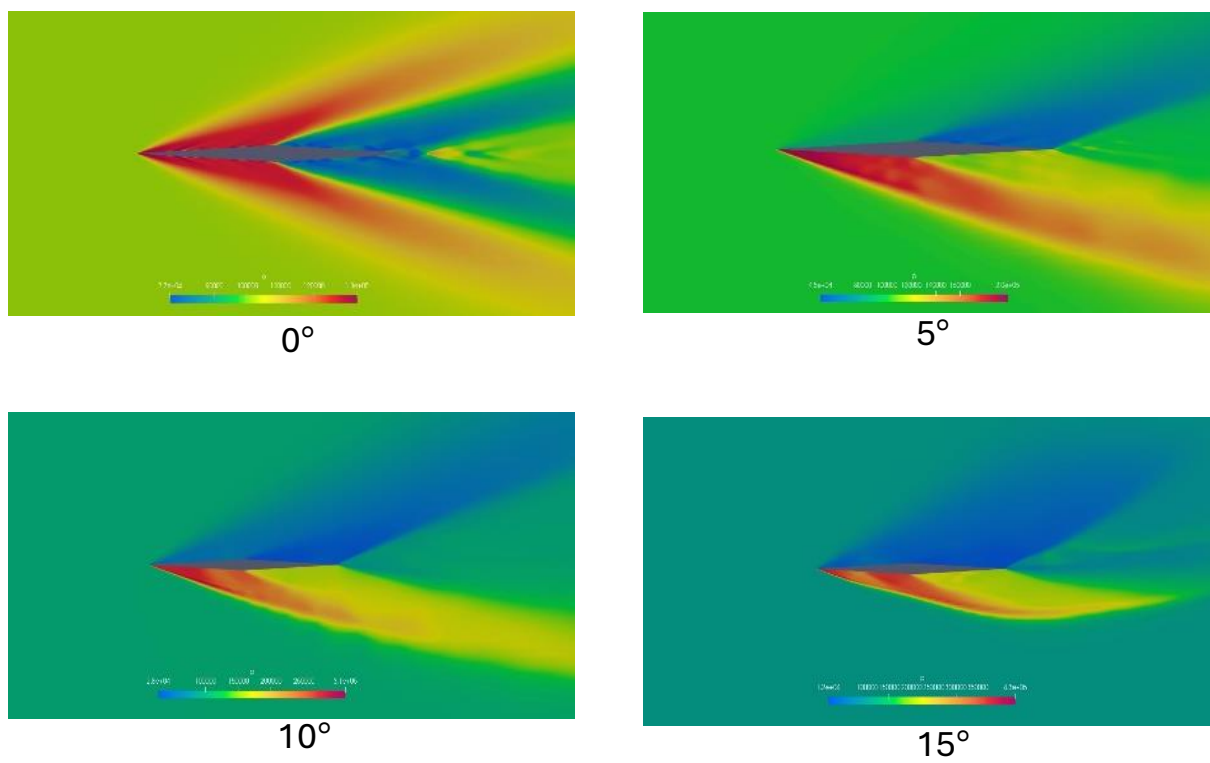


FIGURE 19 : Pressure contour for Mach 3.4 at different Angle of Attack

5.5 Temperature Contours of Double-Wedge Airfoil

Temperature is a critical factor when designing an airfoil, as the materials must withstand high temperatures for extended periods without altering their original shape. While temperature may not be the primary focus in this case, but like pressure, it undergoes significant changes over the airfoil. Post-shock temperatures are higher, while they decrease after passing through the expansion fan. The figure below shows the temperature contours for Mach 1.4, 2.4, and 3.4 at different angles of attack.

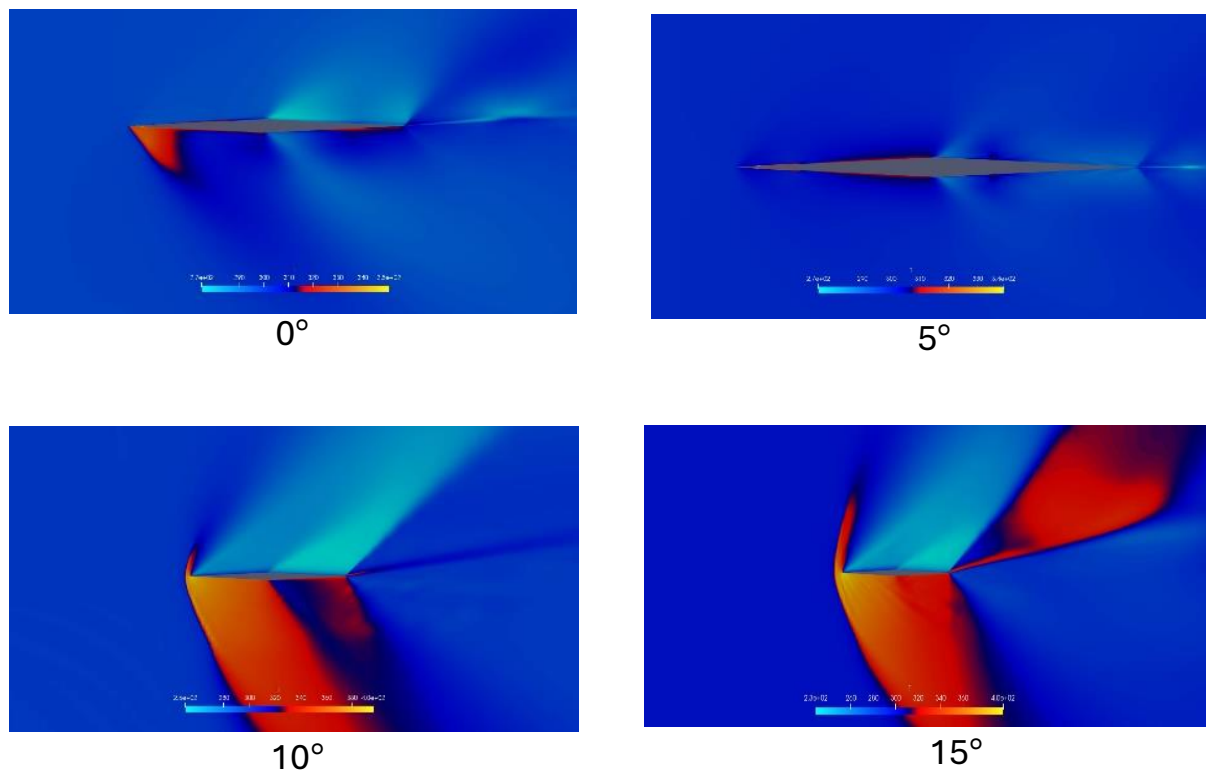
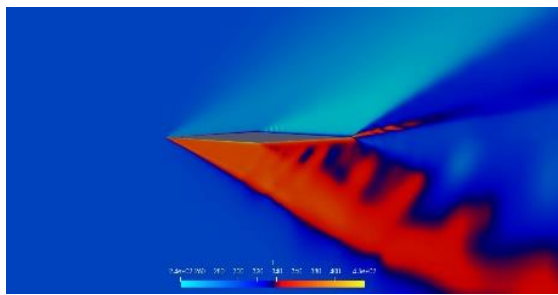
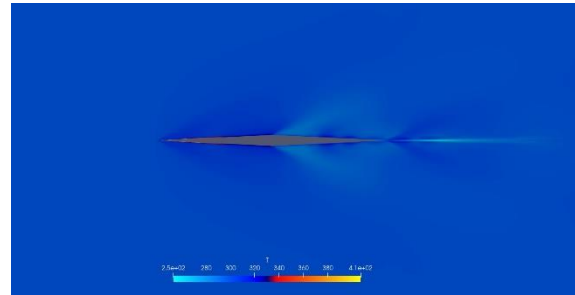


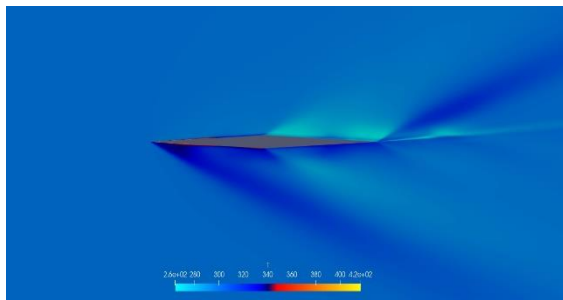
FIGURE 20 : Temperature contour for Mach 1.4 at different Angle of Attack



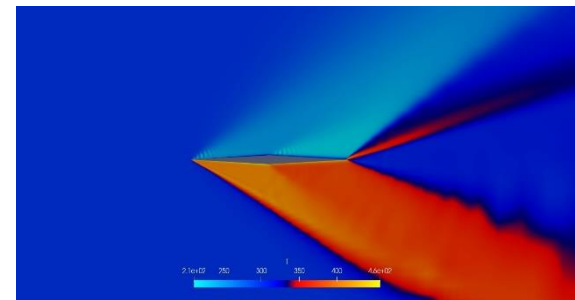
0°



5°

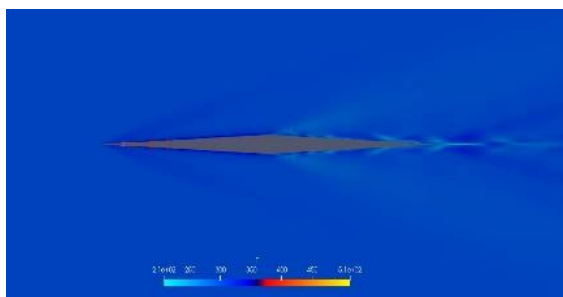


10°

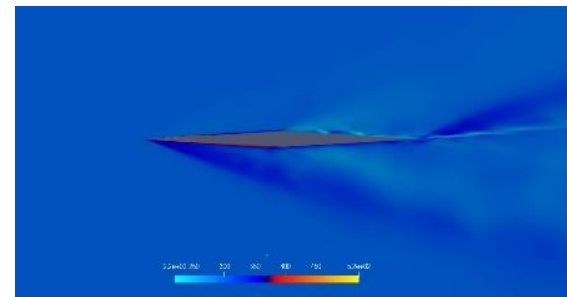


15°

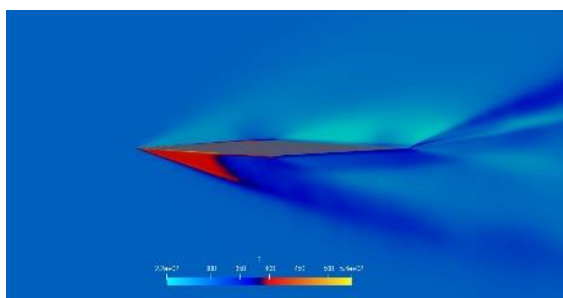
FIGURE 21 : Temperature contour for Mach 2.4 at different Angle of Attack



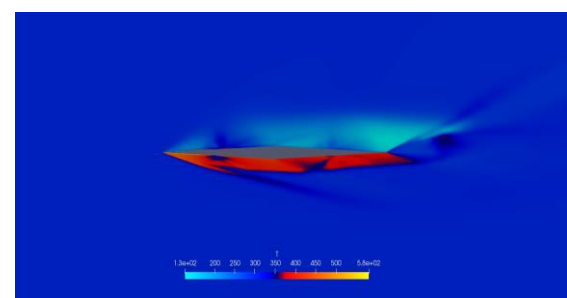
0°



5°



10°



15°

FIGURE 22 : Temperature contour for Mach 3.4 at different Angle of Attack

Conclusion

A numerical study was conducted on a double-wedge airfoil at various Mach numbers and angles of attack. The effects of Mach number and angle of attack on the airfoil were analyzed and compared with the results from an analytical study. Changes in Mach number, pressure distribution, and temperature variation over the airfoil were thoroughly investigated. A mesh independence study was also performed to determine the most computationally efficient yet accurate mesh size. Additionally, the coefficients of drag and lift were obtained and compared. The paper concludes by presenting and comparing the results from the OpenFoam SonicFoam solver with the analytical study, highlighting the errors and differences, and suggesting areas for improvement and further study.

References

- [1] Md. Zulkarna-En, Md. Ashraful Islam, Abdullah Al-Faruk, Islam, R. and Islam, M. (2023). Numerical Analysis of Aerodynamic and Shock Wave Characteristics of Biconvex and Double-Wedge Shape Airfoils for Supersonic Flow. *International Journal of Automotive and Mechanical Engineering*, 20(4), pp.10821–10837.
- [2] John D Anderson Jr, “Modern Compressible Flow” fourth edition, Curator for Aerodynamics, National Air and Space Museum, Smithsonian Institution, and Professor Emeritus of Aerospace Engineering University of Maryland, College Park.
- [3] John D Anderson Jr. “Hypersonic and high-temperature gas dynamics”. American Institute of Aeronautics and Astronautics, 2006.
- [4] Mridu Sai Charan A S, “Supersonic Flow over a Double-Wedge Airfoil” (2020), FOSSEE, IIT-Bombay.
- [5] Sai Pradyumna Reddy Gopavaram & Jyothi Sushma, “Aerodynamic Investigation of Double Wedge Supersonic Airfoil” (2019), ISSN: 2278-0181.
- [6] Chandran. Suren and Karthikeyan. Natarajan, “External Flow Separation”, October 26. 2022
- [7] Luis F. Gutiérrez Marcantonia,b,c, José P. Tamagno,a,d and Sergio A. Elaskara,b,e. “Highspeed flow simulation using OpenFOAM.” In: Asociación Argentina de Mecánica Computacional, 2012.
- [8] Jorge Luis Garrido Tellez et al. “Evaluating Oblique Shock Waves Characteristics on a Double-Wedge Airfoil”. In: Engineering 8.12 (2016), p. 862
- [9] Ruffin, S., and Gupta, A., “Supersonic Channel Airfoils for Reduced Drag”, AIAA Paper 97-0517, Jan. 1997
- [10] Boyd, J. W., Katzen, E. D., and Frick, C. W., "Investigation at Supersonic Speed ($M=1.53$) of the Pressure Distribution over Swept Airfoil of Biconvex Section at Several Angles of Attack," NACA RM A8F22, September, 1948.
- [11] MD, Jahid. Hasan, “A complete learning path for CFD”, May 2022
- [12] Prof Srisha Rao M V, “Gas Dynamis : Fundamental and Applications” IISc Bangalore, NPTEL
- [13] Wentao Yong “Study on Aerodynamic Characteristics of supersonic Airfoils”, February, 2019, <https://doi.org/10.4236/mme.2019.91002>
- [14] The OpenFOAM Foundation : <https://openfoam.org/>
- [15] OpenFOAM userguide : <https://www.openfoam.com/documentation/user-guide>
- [16] SourceForge, a guide to Openfoam guide : <https://foam.sourceforge.net/docs/Guidesa4/OpenFOAMUserGuide-A4.pdf>

